

# Polymer Chemistry

Volume 14  
Number 17  
7 May 2023  
Pages 1993-2136

rsc.li/polymers



ISSN 1759-9962

**PAPER**

Richard Hoogenboom *et al.*

Amidation of methyl ester-functionalised poly(2-oxazoline)s as a powerful tool to create dual pH- and temperature-responsive polymers as potential drug delivery systems



Cite this: *Polym. Chem.*, 2023, **14**, 2034

# Amidation of methyl ester-functionalised poly(2-oxazoline)s as a powerful tool to create dual pH- and temperature-responsive polymers as potential drug delivery systems†

Meike N. Leiske, ‡<sup>a</sup> Ronak Singha,<sup>a</sup> Somdeb Jana,<sup>a</sup> Bruno G. De Geest,<sup>b</sup> and Richard Hoogenboom<sup>†\*</sup><sup>a</sup>

In the past two decades, thermoresponsive polymers based on tertiary amine groups have been studied extensively as a class of dual-responsive polymers. In particular, their temperature-dependent phase transition can be further modulated by the pH value of the environment, rendering them interesting for applications in the biomedical area. In this contribution, we report methyl-ester-functionalised poly(2-alkyl-2-oxazoline)s (PAOx) as a versatile platform for the synthesis of tertiary-amine-functionalised PAOx via straightforward post-polymerisation amidation. The resulting polymers were investigated regarding their stimuli-responsiveness to both, pH value and temperature by turbidimetry measurements. Dynamic light scattering further confirmed the formation of polymeric nanoparticles upon phase separation of block copolymers comprising a responsive polymer block and poly(2-methyl-2-oxazoline) as permanently hydrophilic block. Furthermore, a hydrophobic Rhodamine B derivative was used as model cargo and was found to induce the formation of stable nanoparticles in biological media beyond the responsiveness to pH and temperature of these polymers. Treatment of MDA-MB-231 breast cancer cells with such nanoparticles containing both, the Rhodamine B octadecyl-derivative and paclitaxel, suppressed their proliferation sufficiently *in vitro*. Altogether, PAOx with tertiary amines are presented as versatile materials with interesting characteristics and potential applications in the area of polymeric drug delivery.

Received 15th January 2023,  
Accepted 24th February 2023

DOI: 10.1039/d3py00050h

rs.c.li/polymers

## Introduction

In modern nanomedicine it is a major challenge to deliver therapeutically active agents more safely and directly to the target site.<sup>1,2</sup> Stimuli-responsive polymers have attracted wide attention as smart materials with potential application in the biomedical area,<sup>3–5</sup> e.g., as drug delivery vectors with controlled release properties.<sup>6</sup> External stimuli of interest include pH,<sup>7</sup> temperature,<sup>8</sup> and ionic strength.<sup>4</sup> In particular the response to temperature has been studied comprehensively in the past. Here, two main phenomena have been reported: (i) lower critical solution temperature (LCST)<sup>9</sup> and (ii) upper criti-

cal solution temperature (UCST).<sup>10</sup> While reports on the latter are rare, LCST is a well-studied concept in polymer research. Polymers that possess LCST behaviour include for example *N*-alkyl-substituted polyacrylamides,<sup>11</sup> poly(vinyl methyl ether),<sup>12</sup> poly(*N*-vinylcaprolactam),<sup>13</sup> poly(propylene oxide),<sup>14,15</sup> and poly(2-alkyl-2-oxazoline)s (PAOx).<sup>16,17</sup> In addition to temperature-response, the sensitivity of polymers to changes in pH has been reported to be beneficial for drug delivery applications.<sup>7</sup> In particular, the dynamic protonation of amine-containing polycations has shown promise for tailored cell interactions and endosomal release inside the cells.<sup>3,18</sup> To this end, polymers with tertiary amines in the side chain appear to be interesting as they have been shown to possess a dual responsiveness to both, temperature and pH.<sup>19</sup> While their increased interaction with cell membranes is necessary for efficient polymer uptake, it can also lead to unwanted side-effects, such as increased toxicity or protein fouling.<sup>20</sup> The combination of amine moieties with low- or anti-fouling units is one strategy to circumvent this issue.<sup>21</sup> Polymers of interest include poly(ethylene glycol), poly(amino acid)s, poly(glycerol), poly(acrylamide), poly(vinylpyrrolidone), and PAOx.<sup>22,23</sup>

<sup>a</sup>Supramolecular Chemistry Group, Centre of Macromolecular Chemistry (CMaC), Department of Organic and Macromolecular Chemistry, Ghent University, Krijgslaan 281 S4, B-9000 Ghent, Belgium. E-mail: richard.hoogenboom@ugent.be

<sup>b</sup>Department of Pharmaceutics and Cancer Research Institute Ghent (CRIG), Ghent University, Ottengemsesteenweg 460, B-9000 Ghent, Belgium

† Electronic supplementary information (ESI) available. See DOI: <https://doi.org/10.1039/d3py00050h>

‡ Current address: Faculty of Biology, Chemistry & Earth Sciences, University of Bayreuth, Universitätsstraße 30, 95447 Bayreuth, Germany.

PAOx are a polymer class that is characterised by its large chemical versatility. Besides the possibility to design telechelic PAOx,<sup>24</sup> the synthesis *via* the cationic ring-opening polymerisation (CROP) of 2-oxazolines allows for the preparation of a wide range of side chain functionalised homo- and copolymers,<sup>25–27</sup> as well as different polymer architectures.<sup>28–30</sup> Due to the favourable low-fouling properties<sup>31,32</sup> and low immunogenicity of hydrophilic PAOx,<sup>33–35</sup> they possess high potential for use in the field of nanomedicines and numerous studies have already investigated their potential in this area.<sup>36–39</sup> PAOx with longer alkyl side chains (*e.g.*, ethyl, *n*-propyl, or *iso*-propyl)<sup>40,41</sup> as well as other functional side chains such as methyl esters<sup>42</sup> or nitriles<sup>43</sup> exhibit LCST behavior. In addition, PAOx with ionisable groups have been reported to be responsive to both, pH and temperature.<sup>44,45</sup> Unfortunately, the direct synthesis of PAOx with tertiary amines in the side chain is hampered by the sensitivity of the CROP towards external nucleophiles.<sup>46</sup> Nonetheless, the post-polymerisation modification (PPM) of functional, reactive side chains has facilitated the functionalisation of PAOx with tertiary amines.<sup>47,48</sup> Such synthesis of functional PAOx with different tertiary amines in the side chain *via* PPM allows for a straightforward comparison of the effect of the amino-substituent on the stimuli-responsiveness. To the best of our knowledge, the design and dual-responsiveness of PAOx comprising tertiary amines in the side chain to pH and temperature has not been reported to date.

The aim of this project was the design of nanoparticles based on block copolymers with a dual-responsive PAOx block with tertiary amines in the side chain *via* straightforward amidation of methylester-containing PAOx. Therefore, block copolymers of 2-methyl-2-oxazoline (MeOx) as permanently hydrophilic block and 2-methoxycarbonylpropyl-2-oxazoline (C3MestOx) were prepared and functionalised with different tertiary amines through direct amidation as shown in Scheme 1. The temperature- and pH-response of these polymers was studied by means of turbidity and dynamic light

scattering. The effect of physiologically relevant environments on the thermoresponsive properties was further investigated. Tertiary amine-functionalised block copolymers were used for the preparation paclitaxel-loaded polymeric micelles, which were evaluated regarding their potential to suppress the *in vitro* proliferation of MDA-MB-231 breast cancer cells. Altogether, these tertiary amine-functionalised PAOx are presented as versatile and responsive materials.

## Experimental part

### Materials and instrumentation

**Materials.** The following chemicals were used as received, unless otherwise stated. Barium oxide (BaO, 90%), was purchased from Acros Organics. Methyl *p*-toluenesulfonate (MeOTs, 98%), anhydrous acetonitrile (MeCN, 99%) diethyl-ether (Et<sub>2</sub>O, >99%), and sodium azide were purchased from Sigma-Aldrich. Paclitaxel (Ptx, >98%), octadecyl Rhodamine B chloride (RhB-C18, >95%), Triazabicyclodecene (TBD, >98%), *N,N*-diisopropylethylenediamine (DIPED, >97%), 1-(2-aminoethyl)piperidine (AEP, ≥97%), and 1-isopropylpiperazine (IPP, ≥98%) were obtained from TCI. Dulbecco's phosphate buffered saline (DPBS, Gibco), fetal bovine serum (FBS, Gibco), Dulbecco's Modified Eagle's medium: Nutrient Mixture F-12 (DMEM/F12, Gibco), Trypsin (Gibco), were used as received.

Deuterated dimethylsulfoxide (DMSO-d<sub>6</sub>), and deuterated chloroform (CDCl<sub>3</sub>) were purchased from Eurisotop.

MeOTs and MeCN were further purified by distillation before usage and stored under inert N<sub>2</sub> atmosphere in a glove box. Methoxycarbonylpropyl-2-oxazoline (C3MestOx), a monomer with a propyl (C3) spacer between methyl ester (Mest) and the 2-oxazoline (Ox) ring, was synthesised following a previously reported protocol and was further purified by distillation over BaO,<sup>49</sup> before storage under inert N<sub>2</sub> atmosphere in a glove box.

Deionised water was prepared with a resistivity less than 18.2 MΩ cm using an Arium 611 from Sartorius with the Sartopore 2150 (0.45 + 0.2 μm pore size) cartridge filter.

**<sup>1</sup>H nuclear magnetic resonance (NMR) spectroscopy.** NMR of all samples was carried out using a Bruker AVANCE III HD 300 MHz or 400 MHz spectrometer as indicated utilising deuterated solvents obtained from Sigma-Aldrich.

**Gas chromatography (GC).** GC was employed to evaluate the monomer conversions of oxazolines during CROP. GC was performed in an Agilent 7890A system equipped with a VWR Carrier-160 hydrogen generator and an Agilent HP-5 column of 30 m length and 0.32 mm diameter. Detection was done with a Flame ionization detector (FID). FID detector was set to 280 °C and inlet was set to 250 °C with a split injection of ratio 25 : 1. Hydrogen was used as carrier gas at a flow rate of 2 mL min<sup>-1</sup>. The oven temperature was increased with 20 °C min<sup>-1</sup> from 50 °C to 120 °C, followed by a ramp of 50 °C min<sup>-1</sup> to 300 °C. Conversion was determined based on the integration of monomer peaks using acetonitrile (reaction solvent) as an internal standard.



**Scheme 1** Preparation of polymers used in this study. A: Synthesis of PMeOx<sub>n</sub>-*b*-PC3MestOx<sub>m</sub> *via* cationic ring-opening polymerisation of MeOx (1<sup>st</sup> block) and sequential addition of C3MestOx (2<sup>nd</sup> block), followed by termination with sodium azide. B: Post-polymerisation modification of PMeOx<sub>n</sub>-*b*-PC3MestOx<sub>m</sub>, yielding different tertiary-amine-modified polymers.

**Size-exclusion chromatography (SEC).** SEC was performed on two different systems. SEC of DMAc-soluble polymers was performed on an Agilent 1260-series HPLC system equipped with a 1260 online degasser, a 1260 ISO-pump, a 1260 automatic liquid sampler, a thermostatted column compartment at 50 °C equipped with two PLgel 5 µm mixed-D columns and a mixed-D guard column in series, a 1260 diode array detector, and a 1260 refractive index detector. The used eluent was DMAc containing 50 mM of LiCl at a flow rate of 0.500 mL min<sup>-1</sup>. The spectra were analysed using the Agilent ChemStation software with the SEC add on. Molar mass and dispersity (*D*) values were determined by SEC-analysis, calculated against polymethylmethacrylate (PMMA) standards.

SEC of more hydrophilic, DMAc-insoluble polymers was performed on an Agilent 1260-series HPLC system equipped with an online PSS degasser, a 1260 ISO-pump, a 1260 automatic liquid sampler (ALS), a 1261 thermostatted column compartment (TCC) at 30 °C equipped with two PSS Novema Max 5 µm columns and a precolumn in series, a 1262 diode array detector (DAD) and a 1290 refractive index detector (RID). The used eluent was an acetate buffer at pH 3.6 containing 30% acetonitrile and 0.1 M NaNO<sub>3</sub> at a flow rate of 0.500 mL min<sup>-1</sup>. The spectra were analysed using the Agilent Chemstation software with the GPC add on. Molar mass values and *D* values were calculated against PEG standards from PSS.

**Lyophilisation.** Lyophilisation of samples was conducted using an Alpha 1-2 LDplus freeze-dryer from Martin Christ Gefriertrocknungsanlagen GmbH (Germany).

**pH adjustment.** The pH of polymer-containing solutions in diH<sub>2</sub>O was adjusted using 0.1 M NaOH and HCl solutions. pH measurements were conducted with a digital pH meter.

**Dynamic light scattering (DLS).** DLS was measured on a Zetasizer Nano-ZS Malvern apparatus (Malvern Instruments Ltd) using disposable cuvettes. The excitation light source was a He-Ne laser at 633 nm and the intensity of the scattered light was measured at an angle of 173°. This method measures the rate of intensity fluctuation, and the size of the particles is determined through the Stokes-Einstein equation. If not indicated otherwise, the concentration of the polymer solution was 1 mg mL<sup>-1</sup> (in diH<sub>2</sub>O, DPBS or DMEM/F12). If not stated otherwise, results represent the mean and SD of 5 measurements with 3 runs each.

**Crystal16™ turbidimeter.** Cloud point temperatures were measured on a Crystal16™ parallel crystalliser turbidimeter developed by Avantium Technologies connected to a recirculation chiller and dry compressed air. Aqueous polymer solutions at indicated concentrations were heated from 4 °C to 70 °C with a heating rate of 1.0 °C min<sup>-1</sup> followed by cooling to 4 °C at a cooling rate of 1.0 °C min<sup>-1</sup>. This cycle was repeated three times. The cloud point temperature (*T*<sub>CP</sub>) is reported as the 50% transmittance temperature in the 2<sup>nd</sup> heating run.

## Synthesis and characterisation

### Polymer synthesis

**Homopolymerisation (PC3MestOx<sub>150</sub>).** PC3MestOx was synthesised *via* cationic ring opening polymerisation (CROP). In a

N<sub>2</sub> filled glovebox, C3MestOx (3.00 mL, 17.5 mmol), MeOTs (0.018 mL, 0.12 mmol) and acetonitrile (ACN) (1.357 mL) were added to a 5 mL microwave vial and then polymerised in the Biotage microwave for 23 min at 140 °C. Termination of the polymer was done with sodium azide. Precipitation was done in a ten-fold excess of Et<sub>2</sub>O and the resulting precipitate was isolated *via* centrifugation, dissolved in water and freeze dried.

<sup>1</sup>H NMR (300 MHz, CDCl<sub>3</sub>) of PC3MestOx<sub>150</sub>: δ = 3.58 (3H, s, -CO-O-CH<sub>3</sub>), 3.38 (4H, m, -CH<sub>2</sub>-CH<sub>2</sub>- (backbone)), 2.33 (4H, m, -N-CO-CH<sub>3</sub>- and -CH<sub>2</sub>-CO-O-) 1.84 (2H, m, -CH<sub>2</sub>-CH<sub>2</sub>-) ppm.

SEC data can be found in Table 1.

**Synthesis of block copolymers.** The synthesis of block copolymers is exemplarily described for PMeOx<sub>60</sub>-*b*-PC3MestOx<sub>90</sub>.

Block copolymers were synthesised *via* CROP. In a N<sub>2</sub> filled glovebox, MeOx (0.339 mL, 4.0 mmol), MeOTs (0.010 mL, 0.067 mmol) and MeCN (3.63 mL) were added to a 20 mL microwave vial and then polymerised in the Biotage microwave for 20 min at 140 °C. Prior polymerisation a 100 µL sample was taken for analysis of the conversion *via* GC. After that, the vial was transferred back into the glovebox to withdraw a 200 µL sample for analysis *via* GC, <sup>1</sup>H NMR, and SEC. Subsequently, C3MestOx (1.027 mL, 6.0 mmol) was added to the reaction vial and another 100 µL sample was taken for GC analysis. The reaction mixture was then polymerised at 140 °C for an additional 20 min. After that, the vial was transferred back into the glovebox to withdraw a 200 µL sample for analysis *via* GC, <sup>1</sup>H NMR, and SEC. Purification of the polymers was achieved as described for the homopolymer.

SEC data can be found in Table 1.

**General amidation procedure.** The amidation was performed as previously reported by our group.<sup>50</sup> A solution of polymer (2.5 mmol of ester groups, 1 eq.) in 2 mL anhydrous MeCN was prepared. In a separate vial, a solution of TBD (1.25 mmol, 0.5 eq.) and amine (15 mmol, 6 eq.) and the appropriate volume of MeCN (to obtain a 3 mL solution) was prepared. Next, the solution containing the catalyst and amine was heated to 70 °C in a heating block. After an equilibration time of 5 min, the polymer solution was added. The reaction was stirred overnight. The crude reaction mixture was then purified *via* dialysis against diH<sub>2</sub>O (RC, MWCO 3.5 kDa) for three days with daily water changes. After lyophilisation, the products were obtained as colourless solids. Quantitative functionalisation was verified *via* <sup>1</sup>H NMR spectroscopy. SEC measurements were performed to verify the integrity of the polymers during the functionalisation process.

**Table 1** SEC analysis of C3MestOx-containing (co)polymers *via* SEC in DMAc (PMMA-calibration)

Polymer	<i>M</i> <sub>n</sub> (g mol <sup>-1</sup> )	<i>D</i>
PC3MestOx <sub>150</sub>	29 000	1.17
PMeOx <sub>20</sub> - <i>b</i> -PC3MestOx <sub>130</sub>	29 900	1.15
PMeOx <sub>40</sub> - <i>b</i> -PC3MestOx <sub>110</sub>	23 000	1.27
PMeOx <sub>60</sub> - <i>b</i> -PC3MestOx <sub>90</sub>	26 500	1.18

$^1\text{H}$  NMR (300 MHz, DMSO- $d_6$ ) of PC3DIPEDOX $_{150}$ :  $\delta$  = 7.66 (1H, s,  $-\text{CO}-\text{NH}-\text{CH}_2-$ ), 3.33 (4H, m,  $-\text{CH}_2-\text{CH}_2-$  (backbone)), 2.93 (4H, m,  $-\text{CH}_2-\text{CH}_2-\text{N}-$  and  $\text{CH}_3-\text{CH}-\text{N}-$ ), 2.37 (4H, m,  $-\text{N}-\text{CO}-\text{CH}_3-$  and  $-\text{CH}_2-\text{CO}-\text{NH}-$ ), 2.06 (2H, m,  $-\text{NH}-\text{CH}_2-\text{CH}_2-$ ), 1.69 (2H, m,  $-\text{CH}_2-\text{CH}_2-\text{CH}_2-$ ), 0.93 (12H, d, *b*,  $(\text{CH}_3)_2-\text{CH}-$ ) ppm.

SEC (Table 2):

### Biological assays

**Cell culture.** MDA-MB-231 cells were obtained from ATCC. Cells were grown in DMEM/F12 supplemented with 10% (v/v) FBS, 100 U mL $^{-1}$  penicillin, and 100  $\mu\text{g}$  mL $^{-1}$  streptomycin. Cells were maintained at 37 °C in a fully humidified atmosphere containing 5% CO $_2$ .

**Cell viability.** Cells were cultured as described above. For the cell viability assay, cells (10 $^4$  per well) were seeded in 96-well plates and allowed to adhere overnight. The media was subsequently removed and replaced by fresh, polymer-containing media. Then, the cells were incubated at 37 °C for an additional 24 h. After that, the media was removed, and the cells were washed with 100  $\mu\text{L}$  DPBS. Next, fresh media containing the thiazolyl blue tetrazolium bromide (MTT) (concentration: 1 mg mL $^{-1}$ ) was added (100  $\mu\text{L}$  per well). Note: MTT (50 mg) was dissolved in 10 mL of sterile DPBS, filtrated (membrane, 0.22  $\mu\text{m}$ ), and 1 to 5 diluted in culture medium prior to use in this assay. After incubation at 37 °C for 3 h, 100  $\mu\text{L}$  of DMSO were added to each well and the plates were gently shaken in the dark for 1 h to dissolve the formazan crystals. Quantification was done by measuring the absorbance at  $\lambda$  = 590 nm using a microplate reader. Untreated cells on the same plate served as negative control (100% viability), cells treated with 20% DMSO as positive control (0% viability), and wells without cells as background. Experiments were formed in triplicates on three different plates. The relative cell viability was determined by eqn (1).

$$\% \text{Cell viability} = \frac{\text{Abs. sample} - \text{Abs. background}}{\text{Abs. negative control} - \text{Abs. background}} \times 100 \quad (1)$$

### Cell growth inhibition assays

Cell growth inhibition assays were conducted as previously reported.<sup>51</sup> The following alterations were made to the MTT

protocol described in ref. 51. Cells were seeded at a density of  $3 \times 10^3$  cells per well. One plate was used for each time point. Media was changed daily. After the indicated time points (0, 1, 2, or 3 days), (polymer-containing) cell medium was removed, and cells were gently washed with 100  $\mu\text{L}$  of DPBS before the addition of fresh medium containing the MTT reagent as described in ref. 51 and incubated for 3 h at 37 °C. The relative cell growth was determined by eqn (2) and (3).

$$\text{Cell growth} = \frac{(\text{absorbance}(\text{sample or control}) - \text{absorbance}(\text{blank}))}{\text{absorbance}(\text{blank})} \quad (2)$$

$$\text{Relative cell growth} = \frac{\text{cell growth}(\text{sample or control day } n)}{\text{cell growth}(\text{control day } 0)} \quad (3)$$

### Statistical analysis

All data plotted with error bars are expressed as means with standard deviation. The *P* values were generated by analysing data with a one-way ANOVA and Turkey test using OriginLab.

## Results and discussion

The aim of this study was the development of dual-responsive tertiary amine-modified PAOX (co)polymers.

### Synthesis of amine-modified block copolymers

2-oxazoline monomers with tertiary amino groups cannot be polymerised *via* CROP. However, they can be introduced into the polymers *via* post-polymerisation modification (PPM), *e.g.*, the amidation of ester groups.<sup>47,48</sup> The CROP of functional 2-oxazolines enables the preparation of well-defined methyl-ester-functionalised homo- and co-polymers (Scheme 1A).<sup>42</sup>

We prepared four block copolymers (BCPs) with a varying ratio of C3MestOx and the non-ionic stealth monomer MeOx: (i) PC3MestOx $_{150}$ , (ii) PMeOx $_{20}$ -*b*-PC3MestOx $_{130}$ , (iii) PMeOx $_{40}$ -*b*-PC3MestOx $_{110}$ , and (iv) PMeOx $_{60}$ -*b*-PC3MestOx $_{90}$ . All polymers featured narrow dispersity ( $D \leq 1.27$ , Table 1) and were subsequently modified with *N,N*-diisopropylethylenediamine (DIPED) *via* post-polymerisation amidation using TBD as a catalyst (Scheme 1B).<sup>48,50</sup> The reactions proceeded quantitatively and yielded the polymers PC3DIPEDOX $_{150}$ , PMeOx $_{20}$ -*b*-PC3DIPEDOX $_{130}$ , PMeOx $_{40}$ -*b*-PC3DIPEDOX $_{110}$ , and PMeOx $_{60}$ -*b*-PC3DIPEDOX $_{90}$  as confirmed *via*  $^1\text{H}$  NMR spectroscopy (Fig. S1†) by the disappearance of the methyl ester peak at  $\delta$  = 3.58 ppm and the appearance of the characteristic diisopropyl peaks (H10) at  $\delta$  = 0.93 ppm. SEC measurements further verified the integrity of the polymer chains during the amidation process (Table 2 and Fig. S2†).

### Temperature-responsiveness

Next, the responsiveness of the prepared polymers to pH and temperature was studied by turbidimetry at different pH values (Fig. 1A and S3, Tables S1 to S6†). At pH 9 PC3DIPEDOX $_{150}$  had

**Table 2** Characterisation of amine-modified block copolymers *via* SEC measurements

Polymer	$M_n$ (g mol $^{-1}$ )	$D$
PC3DIPEDOX $_{150}$	36 600 <sup>a</sup>	1.26 <sup>a</sup>
PMeOx $_{20}$ - <i>b</i> -PC3DIPEDOX $_{130}$	38 600 <sup>a</sup>	1.24 <sup>a</sup>
PMeOx $_{40}$ - <i>b</i> -PC3DIPEDOX $_{110}$	33 700 <sup>a</sup>	1.25 <sup>a</sup>
PMeOx $_{60}$ - <i>b</i> -PC3DIPEDOX $_{90}$	27 400 <sup>a</sup>	1.34 <sup>a</sup>
PMeOx $_{60}$ - <i>b</i> -PC3AEPOX $_{90}$	32 200 <sup>a</sup>	2.56 <sup>a</sup>
	22 600 <sup>b</sup>	1.12 <sup>b</sup>
PMeOx $_{60}$ - <i>b</i> -PC3IPPOX $_{90}$	22 400 <sup>a</sup>	1.30 <sup>a</sup>

<sup>a</sup> SEC measurements in DMAc (PMMA calibration). <sup>b</sup> SEC measurements in acetate buffer at pH 3.6 containing 30% (v/v) MeCN and 0.1 M NaNO $_3$  (PEG calibration).

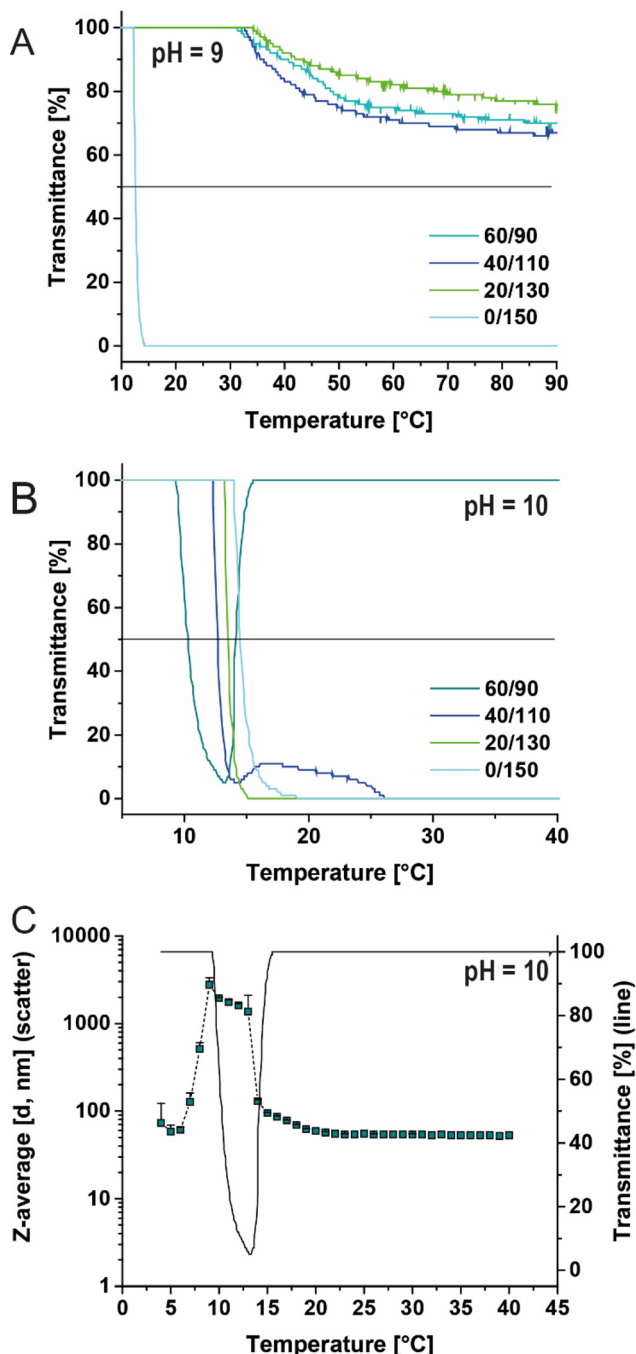


**Fig. 1** Response of C3DIPEDOX-containing (co)polymers to pH value and temperature. Polymer concentration: 5 mg mL<sup>-1</sup> in diH<sub>2</sub>O. Z-average was determined via DLS measurements. Transmittance was determined via turbidimetry measurements (Crystal16™). A and B: Turbidimetry curves of PC3DIPEDOX<sub>150</sub>, PMeOx<sub>20</sub>-*b*-PC3DIPEDOX<sub>130</sub>, PMeOx<sub>40</sub>-*b*-PC3DIPEDOX<sub>110</sub>, and PMeOx<sub>60</sub>-*b*-PC3DIPEDOX<sub>90</sub> at pH9 (A) and at pH 10 (B). C: overlay of temperature-dependent Z-average and transmittance of PMeOx<sub>60</sub>-*b*-C3DIPEDOX<sub>60</sub> at pH = 10.

a very low  $T_{CP}$  of 12.1 °C, while none of the three BCPs showed visible aggregates up to 90 °C (Fig. 1A). Interestingly, at pH 10, all investigated polymers featured temperature responsiveness (Fig. 1B). While the  $T_{CP}$  of PC3DIPEDOX<sub>150</sub> did not change sig-

nificantly compared to pH 9, a drastic decrease in  $T_{CP}$  was observed for all BCPs. Strikingly, at the same weight concentration (5 mg mL<sup>-1</sup>) the  $T_{CP}$  decreased in the following order: PC3DIPEDOX<sub>150</sub> (15 °C) > PMeOx<sub>20</sub>-*b*-PC3DIPEDOX<sub>130</sub> (14 °C) > PMeOx<sub>40</sub>-*b*-PC3DIPEDOX<sub>110</sub> (13 °C) > PMeOx<sub>60</sub>-*b*-PC3DIPEDOX<sub>90</sub> (10 °C), indicating that block copolymers with a larger hydrophilic block phase separated at a slightly lower temperature. At this point, it is noteworthy to mention, that the  $T_{CP}$  determination of individual polymers underlies some experimental uncertainty due to individual pH adjustments. However, different measurements revealed the same trend as reported above (data not shown). While the introduction of hydrophilic end-groups or blocks into temperature-responsive polymers generally leads to an increase of the  $T_{CP}$ ,<sup>8,52</sup> we assume that in the present case aggregate formation is facilitated by more efficient shielding and phase separation of the temperature-responsive block from the hydrophilic block. In addition, upon increasing the temperature above the  $T_{CP}$  (13 °C), the transmittance of PMeOx<sub>60</sub>-*b*-PC3DIPEDOX<sub>90</sub> further increased to 100%, suggesting the formation of smaller nanostructures by fragmentation of the large aggregates.<sup>53–55</sup> To gain further insight into this process, temperature-dependent DLS measurements of this polymer (PMeOx<sub>60</sub>-*b*-PC3DIPEDOX<sub>90</sub>) were performed at different pH values and correlated to the observed turbidimetry profiles (Fig. 1C and Fig. S3†). At pH 9, no temperature-induced formation of aggregates or defined spherical structures was observed (Fig. S3A†), corroborating with the absence of a  $T_{CP}$ , due to protonation of the tertiary amines. In contrast, at pH 10, a sudden increase of the z-average was observed around 9 °C from 50 nm (at 4 °C) to >2000 nm (at 10 °C), which is very close to the  $T_{CP}$  at 10 °C from turbidimetry. However, at 14 °C, the z-average sharply decreased to 130 nm, and upon further heating, it stabilised at 55 nm. The heat-induced formation of stable PMeOx<sub>60</sub>-*b*-PC3DIPEDOX<sub>90</sub> nanoparticles (NPs) was in agreement with the  $T_{CP}$  measurements (Fig. 1C), indicating a dehydration of the amine-containing NP core and a stabilisation by the hydrophilic PMeOx corona. The low polydispersity index (PDI) of 0.15 further confirmed the presence of narrow disperse polymer NPs. Further increasing the pH to 11 led to an acceleration of this effect (Fig. S3B†), due to increased hydrophobicity of the DIPEDOX units at lower degree of protonation. In contrast to PMeOx<sub>60</sub>-*b*-PC3DIPEDOX<sub>90</sub>, the remaining PC3DIPEDOX-containing other copolymers did not form spherical structures of small size and low PDI upon heating at pH 10 (Fig. S4†), which we attribute to an unfavourable hydrophobic–hydrophilic ratio.<sup>56</sup>

While these results provided important information about the pH-dependent temperature-responsiveness of the prepared polymers, all suitable pH values were far outside the physiological range. For this reason, the stimuli-responsiveness was studied in Dulbecco's phosphate-buffered saline (DPBS) and cell culture media (DMEM/F12) (Fig. S5†). We assumed that the presence of ions, sugars, and amino acids will have a major impact on the temperature-responsiveness of the prepared polymers. While the effect of salts and ions on the temp-

erature-induced phase transition of thermoresponsive polymers has been widely studied,<sup>57,58</sup> investigations using more complex cell culture media are less commonly studied in the literature.<sup>59</sup> In DPBS, a  $T_{CP}$  for all DIPEDOX-containing (co) polymers was observed, triggered by the salting out effects of the buffer.<sup>58,60</sup> Interestingly, an even more pronounced difference between the homopolymer PC3DIPEDOX<sub>150</sub> ( $T_{CP}$  = 50 °C) and the BCPs ( $T_{CP}$  = 20–25 °C) was found (Fig. S5A and Table S1†). PMeOx<sub>60</sub>-*b*-PC3DIPEDOX<sub>60</sub> showed turbidity between 22 and 25 °C, however, the  $T_{CP}$  could not be calculated due to a subsequent clearing up of the solution due to the formation of smaller nanoparticles from PMeOx<sub>60</sub>-*b*-PC3DIPEDOX<sub>90</sub> as was verified *via* DLS measurements (Fig. S5C†). At temperatures above 30 °C, NPs with a diameter of 70 nm and a PDI of 0.2 were formed. Unfortunately, in DMEM/F12, the  $T_{CP}$  of all BCPs was higher than 40 °C (Fig. S4B†). Consequently, nanoparticles did not form at physiological temperature in cell-culture conditions.

In a next step, the effect of the nature of the different tertiary amines on the  $T_{CP}$  and self-assembly behaviour was studied. In addition, to DIPED, AEP and IPP were chosen as modification agents to further lower the  $T_{CP}$ , as previously reported for similar structures.<sup>19</sup> For this purpose, different tertiary amine modified PMeOx<sub>60</sub>-*b*-PC3MestOx<sub>90</sub>-copolymers were compared (Scheme 1B): (i) methoxycarbonylpropyl-2-oxazoline (C3MestOx; control polymer), (ii) DIPED-modified C3MestOx (C3DIPEDOX), (iii) IPP-modified C3MestOx (C3IPPOx), and (iv) AEP-modified C3MestOx (C3AEPOx) (Fig. 2 and Table S1†). PMeOx<sub>60</sub>-*b*-PC3MestOx<sub>90</sub> possessed a  $T_{CP}$  of 25 °C in both, DPBS and DMEM/F12, emphasising its inertness to environmental changes. In contrast, all tertiary amine-functionalised PAOx showed an increased  $T_{CP}$  in DMEM/F12 when compared to DPBS, potentially caused by the additional sugars and amino acids in the cell culture media, which could impact the protonation and consequently the hydrophobicity of the tertiary amines of the polymer.<sup>61</sup> Unfortunately, none of the amine-functionalised copolymers possessed a  $T_{CP}$  below 37 °C, supposedly rendering them unsuitable for applications that require assembled particles in cell culture media. Nonetheless, their suitability as drug carriers in cell culture media was further evaluated as shown in the following paragraphs.

### Preparation of nanoparticles

In a next step, the amine-functionalised BCPs PMeOx<sub>60</sub>-*b*-PC3DIPEDOX<sub>90</sub>, PMeOx<sub>60</sub>-*b*-PC3AEPOx<sub>90</sub>, and PMeOx<sub>60</sub>-*b*-PC3IPPOx<sub>90</sub> as well as the C3MestOx-containing BCP PMeOx<sub>60</sub>-*b*-PC3MestOx<sub>90</sub> were applied for the preparation of nanoparticles (NPs) *via* the thin-layer assembly method.<sup>43,62</sup> In this method, BCPs are commonly dissolved in an unspecific solvent, which features a low boiling point (*e.g.*, methanol) and added to a glass vial. After that, the BCPs are rehydrated in a solvent, which specifically dissolves only one block and, consequently, facilitates self-assembly of BCPs. Since in this study NPs will be exposed to cell culture media during biological experiments, we attempted the preparation of NPs directly

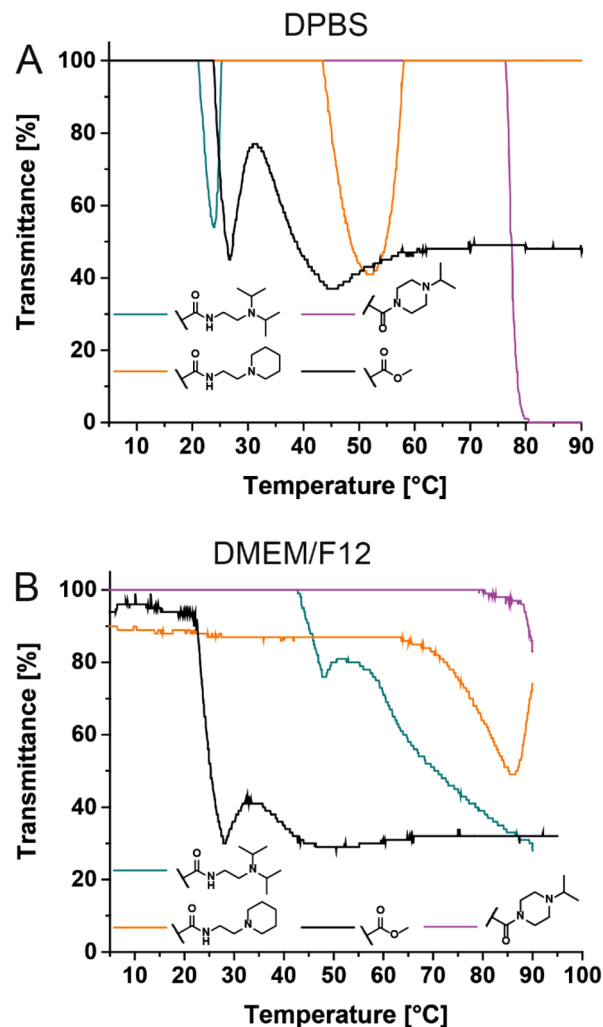
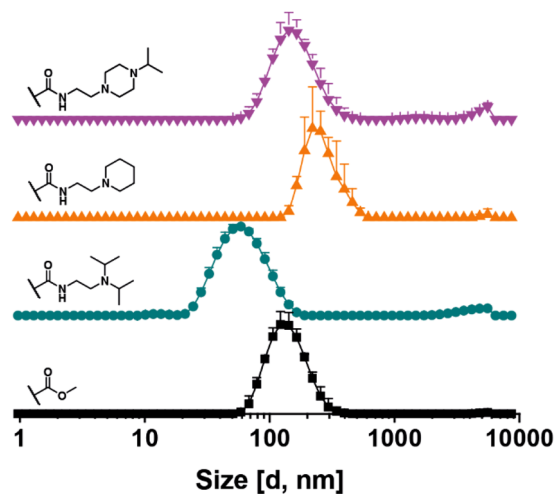


Fig. 2 Temperature-dependent turbidity of different amine- and methyl ester-modified (co)polymers in DPBS (A) and DMEM/F12 (B). Polymer concentration: 5 mg mL<sup>-1</sup>. Transmittance was measured *via* UV vis measurements (Crystal16™).

in DMEM/F12. To this end, the preparation of bare NPs other than those using PMeOx<sub>60</sub>-*b*-C3MestOx<sub>90</sub> was not successful (data not shown). The incompatibility of these polymers with the NP preparation process was assumed to be related to their high  $T_{CP}$  in DMEM/F12 leading to solubilisation of individual polymer chains rather than the formation of NPs. For this reason, a hydrophobic Rhodamine B octadecyl-derivative (RhB-C18) was introduced as a model cargo during NP assembly, assuming that the association of the copolymers with the dye during the preparation process might contribute to the NP assembly process and the stabilisation of the produced NPs, as previously observed for other systems.<sup>43,62–64</sup> Within this study, 5 wt% RhB-C18 with respect to the polymer mass was chosen to prepare NPs *via* the thin-layer assembly method. The success of the assembly process was already visually observed by the pink colour of the NP solution and the absence of visible precipitates. DLS measurements verified the formation of NPs with unimodal size distribution (Fig. 3A).

## A 5wt% RhB-C18



## B 5wt% RhB-C18 + 5wt% Ptx

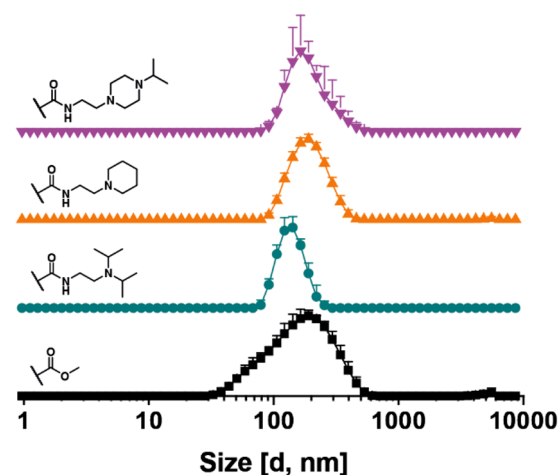


**Fig. 3** Size-distribution of polymer NPs. NPs were prepared from polymers and cargos at indicated concentrations via thin-film assembly in DMEM/F12 at 37 °C. NPs were analysed via DLS measurements at 37 °C (3 measurements with 3 runs each). Polymer concentration: 1 mg mL<sup>-1</sup>. A: 5 wt% RhB-C18; B: 5 wt% RhB-C18 + 5 wt% Ptx.

The size of the NPs depended on the amine-functionality of the polymer (Table S7<sup>†</sup>). DIPEDOX-functionalised polymers formed the smallest NPs ( $d = 57 \pm 1$  nm). In contrast, AEPOX- and IPPOX-modified polymers produced larger NPs ( $d_{\text{AEPOX}} = 303 \pm 27$  nm,  $d_{\text{IPPOX}} = 164 \pm 5$  nm). As the tertiary amine derivatives have a similar molar mass, the volume fraction of the hydrophobic block is similar for all tertiary-amine-containing block copolymers. Hence, the rigidity of the amine-moiety might have an impact on the packing density in the core and, thus, the hydrodynamic diameter of the derived NPs. Unfortunately, attempts to self-assemble the block copolymers in presence of the slightly hydrophobic drug paclitaxel (Ptx) instead of RhB-C18 failed with all amine-functionalised polymers (data not shown).

At this point, it was concluded that the interaction of the more hydrophobic RhB-C18 with the tertiary amines of the polymers is stronger compared to Ptx, which is potentially attributed to the drug's tendency to crystallise in solution combined with a low affinity to the polymers.<sup>65</sup> In contrast, the encapsulation of RhB-C18 could *e.g.* be facilitated hydrophobic interactions, or hydrogen bonding between the functionalities of the polymers and the dye. For this reason, NPs were prepared with a dual loading of 5 wt% RhB-C18 and 5 wt% Ptx. Unlike the attempts with Ptx only, no visible precipitate was observed during the dual-loading process. DLS measurements confirmed the presence of unimodally distributed NPs (Fig. 3B and Fig. S6<sup>†</sup>). Interestingly, the NPs prepared with a dual loading revealed a very similar z-average ( $d \approx 145$  to 185 nm) and PDI (PDI  $\approx 0.2$ ) (Table S7<sup>†</sup>), rendering them suitable for further investigations.

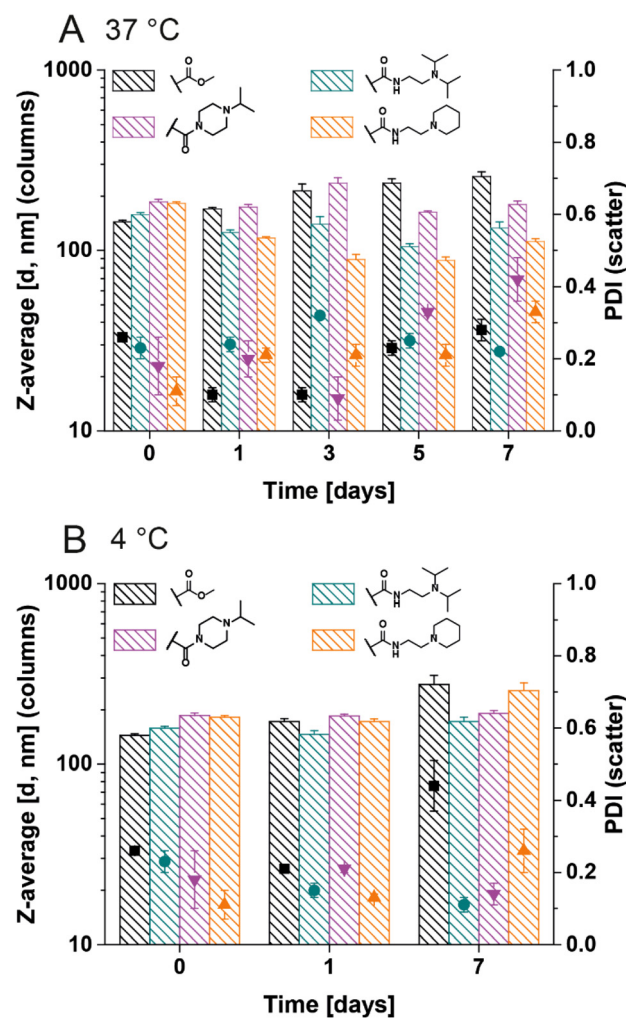


**Fig. 4** Stability of NPs over time at different temperatures. Size and PDI of NPs was determined via DLS measurements at 37 °C (3 measurements with 3 runs each). NPs containing 5 wt% RhB-C18 + 5 wt% Ptx were prepared at 1 mg mL<sup>-1</sup> polymer concentration in DMEM/F12 and incubated for indicated times at A: 37 °C or B: 4 °C.

In a next step, the stability of dual responsive NPs at different temperatures was studied to confirm their applicability for drug delivery. Within this study, 37 °C (human body

temperature) and 4 °C (typical storage temperature) were chosen for a stability study of a duration of one week. The stability of NPs was analysed *via* DLS measurements (Fig. 4).



**Fig. 5** Relative cell growth of MDA-MB-231 breast cancer cells in the presence of NPs. The cells were treated with 100  $\mu$ L of cell culture media containing indicated doses of PtX/polymer. Media was changed daily and supplied with compounds as indicated. Cell growth was determined by MTT assay with initial cell seeding of 3000 cells per well. \*\*\* $p < 0.00005$ . ns: not significant at  $p < 0.005$ . Significances are relative to control and determined *via* one-way ANOVA with Tukey's test.

Despite their high  $T_{CP}$ , the C3IPPOx- and C3DIPEDOx-modified block polymers were also stable at 4 °C for one week. In contrast, the size and dispersity of C3AEPOx-functionalised polymers increased slightly at day 7 ( $d = 252 \pm 2$  nm), potentially due to lower interaction with RhB-C18. Interestingly, the unmodified PMeOx<sub>60</sub>-*b*-PC3MestOx<sub>90</sub>, showed the poorest stability with a significant increase in both, size ( $276 \pm 35$  nm) and PDI ( $0.44 \pm 0.07$ ). We assume this is attributed to the ester-functionality of the polymer, which is not pH-responsive and may interact with the cargo to a lesser extent.

### *In vitro* cytotoxicity of NPs

After the verification of the stability of the prepared NPs, their potential to serve as drug delivery vectors was studied. Due to the intrinsic cytotoxicity of the amine-functionalised polymers, an initial MTT assay of the bare polymers was performed to examine the cytocompatibility and the 50% cytotoxic concentration ( $CC_{50}$ ) (Fig. S7†) in MDA-MB-231 breast cancer cells. The PMeOx block did not enhance cellular compatibility of the amine-functionalised BCPs. The PMeOx<sub>*n*</sub>-*b*-C3DIPEDOx<sub>*m*</sub> BCPs with varying block ratio revealed  $CC_{50}$  values of 0.2 to 0.6  $\mu\text{mol mL}^{-1}$  of amine (70 to 150  $\mu\text{g mL}^{-1}$  polymer) in no specific order (Fig. S7A and Table S8†). These results reflected the absence of a  $T_{CP}$  and respective self-assembly which could shield potential charges.<sup>66</sup> Next, the  $CC_{50}$  values of BCPs with different amine substituents were studied (Fig. S7B†). PMeOx<sub>60</sub>-*b*-PC3MestOx<sub>60</sub> revealed low cytotoxicity as indicated by the  $CC_{50}$  value above all tested concentrations ( $CC_{50(\text{polymer})} > 512 \mu\text{g mL}^{-1}/CC_{50(\text{ester})} > 3.5 \mu\text{mol mL}^{-1}$ ). In comparison, PMeOx<sub>60</sub>-*b*-C3DIPEDOx<sub>90</sub> ( $CC_{50(\text{polymer})} = 126 \mu\text{g mL}^{-1}/CC_{50(\text{amine})} = 0.4 \mu\text{mol mL}^{-1}$ ) and PMeOx<sub>60</sub>-*b*-C3AEPOx<sub>90</sub> ( $CC_{50(\text{polymer})} = 26 \mu\text{g mL}^{-1}/CC_{50(\text{amine})} = 0.1 \mu\text{mol mL}^{-1}$ ) were less tolerated by MDA-MB-231 breast cancer cells. Interestingly, PMeOx<sub>60</sub>-*b*-C3IPPOx<sub>90</sub> possessed the highest cytocompatibility as indicated by its  $CC_{50}$  value ( $CC_{50(\text{polymer})} > 800 \mu\text{g mL}^{-1}/CC_{50(\text{amine})} > 7.0 \mu\text{mol mL}^{-1}$ ).

After the initial evaluation of the bare polymers, NPs containing either 5 wt% RhB or 5 wt% RhB co-encapsulated with 5 wt% Ptx were tested on MDA-MB-231 breast cancer cells to study the potential to deliver a cytostatic agent. While Ptx, a hydrophobic cytoskeletal drug, has very low bioavailability in unformulated form due to its poor water-solubility,<sup>67</sup> the encapsulation into carrier systems, such as polymer NPs or liposomes has shown great promise to improve its efficacy.<sup>65</sup> Here, the therapeutic efficiency of Ptx-loaded NPs was studied to gain insight into the suitability of amine-containing BCPs as carrier systems. Due to its low  $T_{CP}$  of 25 °C in DMEM/F12 (Fig. 2B and Table S1†), the ester-functionalised polymer PMeOx<sub>60</sub>-*b*-C3MestOx<sub>90</sub> served as control polymer (Fig. S8A†). It was further assumed that the absence of pH-responsive units reduces the membrane interaction of this polymer<sup>68</sup> and, consequently, the endosomal release of the therapeutic agent.<sup>18</sup> A preliminary testing *via* an MTT assay was conducted (Table S8 and Fig. S8†). The  $CC_{50}$  value of Ptx delivered with PMeOx<sub>60</sub>-*b*-C3MestOx<sub>90</sub> NPs was found to be 0.36 nmol mL<sup>-1</sup>, however, even at Ptx concentrations of 16 nmol mL<sup>-1</sup> the cell

viability did not decrease below 40%. Noteworthy, the cell viability of Ptx-loaded NPs follows the same slightly decreasing trend as RhB-loaded NPs and bare polymers, indicating an effect of the polymer itself at high concentrations. To this end, PMeOx<sub>60</sub>-*b*-C3DIPEDOx<sub>90</sub> and PMeOx<sub>60</sub>-*b*-C3AEPOx<sub>90</sub> showed a similar trend (Fig. S8B and S8D†). A cytotoxic effect of Ptx-loaded NPs was only observed above the  $CC_{50}$  value of the bare polymer and RhB-containing NPs. These results indicate a high stability of the NPs and, thus, a limited therapeutic potential. Interestingly, Ptx-loaded NPs of PMeOx<sub>60</sub>-*b*-C3IPPOx<sub>90</sub> possessed the lowest  $CC_{50(\text{Ptx})}$  value (0.06 nmol mL<sup>-1</sup>) and a minimum cell viability of 40% (Fig. S8C†). While the low  $CC_{50}$  value is considered favourable for the therapeutic success of the nanocarriers, a further reduction of viable cells would be advantageous.

In a subsequent three-day MTT assay, the long-term effect of Ptx-loaded stimuli-responsive NPs was investigated (Fig. 5). It was found that the growth of MDA-MD-231 breast cancer cells can be suppressed significantly ( $p < 0.00005$ ) *in vitro* by daily treatment with Ptx-containing NPs at drug concentrations as low as 0.25 nmol mL<sup>-1</sup> (Fig. 5E). The results further confirmed the increased cytotoxicity of C3AEPOx- and C3DIPEDOx-functionalised copolymers by a reduction of the cell growth rate through control NPs without Ptx (Fig. 5B and D). While at the lowest investigated concentration, no polymer toxicity was observed (Fig. 5F), it is likely that longer treatment times would also reveal an effect of the polymers themselves. Out of the herein investigated stimuli-responsive polymers, C3IPPOx-functionalised polymers represent the safest alternative for the delivery of cytostatic agents. While the non-responsive C3MestOx-containing NPs revealed similar *in vitro* therapeutic efficiency, the applicability of these NPs is assumed to be hampered by their lower stability as mentioned previously (Fig. 4). Altogether, this preliminary *in vitro* cytotoxicity study revealed that PAOx with tertiary amines in the side chain represent a feasible option for stimuli-responsive polymers with potential application opportunities in the drug delivery area.

## Conclusions

The post-polymerisation amidation of PAOx with methyl ester functionality was applied to yield PAOx with various tertiary amines in the side chain. Block (co)polymers with different amine-content were prepared and studied regarding their solution response to temperature and pH value. The use of buffer systems with relevance for biological experiments provided insight into the complexity of the design of stimuli-responsive polymer NPs for applications in drug delivery. The encapsulation of a hydrophobic Rhodamine B derivative further mediated stable NP formation in cell culture media, emphasising the importance of the suitability of the cargo for the preparation of drug- or dye-loaded polymeric NPs. Paclitaxel-loaded NPs showed cytostatic effects on MDA-MB-231 breast cancer cells, which was associated to the chemistry of the tertiary amine in the polymer side chain. The current results empha-

size the potential of amine-functionalised stimuli-responsive PAOx for drug delivery applications as well as the importance of library approaches for the development of polymer therapeutics.

## Author contributions

M. N. L.: data curation, formal analysis, investigation, methodology, project administration, supervision, visualisation, writing – original draft. R. S.: data curation, formal analysis, investigation, writing – review & editing. S. J.: formal analysis, investigation, supervision, writing – review & editing. B. D. G.: funding acquisition, writing – review & editing. R. H.: conceptualisation, funding acquisition, supervision, writing – review & editing.

## Conflicts of interest

R. H. is one of the founders of Avroxa BV that commercialises poly(2-oxazoline)s as Ultroxa®. The other authors have no conflicts to declare.

## Acknowledgements

R. H. and B. D. G. acknowledge continuous financial support from the Research Foundation – Flanders (FWO) and Ghent University (BOF). We thank Annabelle Mussly, Luna De Ridder and Joren Plaskie for their assistance with polymer preparations.

## References

- 1 R. Duncan and M. J. Vicent, *Adv. Drug Delivery Rev.*, 2013, **65**, 60–70.
- 2 R. Duncan and R. Gaspar, *Mol. Pharmaceutics*, 2011, **8**, 2101–2141.
- 3 D. Schmaljohann, *Adv. Drug Delivery Rev.*, 2006, **58**, 1655–1670.
- 4 M. C. García, in *Stimuli Responsive Polymeric Nanocarriers for Drug Delivery Applications*, ed. A. S. H. Makhlof and N. Y. Abu-Thabit, Woodhead Publishing, 2019, pp. 393–409.
- 5 A. S. Hoffman, *Adv. Drug Delivery Rev.*, 2013, **65**, 10–16.
- 6 P. Bawa, V. Pillay, Y. E. Choonara and L. C. du Toit, *Biomed. Mater.*, 2009, **4**, 022001.
- 7 G. Kocak, C. Tuncer and V. Bütün, *Polym. Chem.*, 2017, **8**, 144–176.
- 8 R. Hoogenboom, in *Smart Polymers and their Applications (Second Edition)*, ed. M. R. Aguilar and J. San Román, Woodhead Publishing, 2019, pp. 13–44.
- 9 V. Aseyev, H. Tenhu and F. M. Winnik, in *Self Organized Nanostructures of Amphiphilic Block Copolymers II. Advances in Polymer Science*, ed. A. Müller and O. Borisov, Springer, Berlin, Heidelberg, 2010, pp. 29–89.
- 10 J. Seuring and S. Agarwal, *Macromol. Rapid Commun.*, 2012, **33**, 1898–1920.
- 11 N. A. Platé, T. L. Lebedeva and L. I. Valuev, *Polym. J.*, 1999, **31**, 21–27.
- 12 U. V. Nikulova and A. E. Chalykh, *Polymers*, 2020, **12**, 2445.
- 13 J. Liu, A. Debuigne, C. Detrembleur and C. Jerome, *Adv. Healthcare Mater.*, 2014, **3**, 1941–1968.
- 14 R. Liu, M. Fraylich and B. R. Saunders, *Colloid Polym. Sci.*, 2009, **287**, 627–643.
- 15 P. Alexandridis, *Curr. Opin. Colloid Interface Sci.*, 1997, **2**, 478–489.
- 16 R. Hoogenboom, *Eur. Polym. J.*, 2022, **179**, 111521.
- 17 M. Hijazi, M. Schmidt, H. Xia, J. Storkmann, R. Plothe, D. D. Santos, U. Bednarzick, C. Krumm and J. C. Tiller, *Polymer*, 2019, **175**, 294–301.
- 18 T. Bus, A. Traeger and U. S. Schubert, *J. Mater. Chem. B*, 2018, **6**, 6904–6918.
- 19 B. Pang, Y. Yu and W. Zhang, *Macromol. Rapid Commun.*, 2021, **42**, 2100504.
- 20 H. Lv, S. Zhang, B. Wang, S. Cui and J. Yan, *J. Controlled Release*, 2006, **114**, 100–109.
- 21 Z. Ma, S. W. Wong, H. Forgham, L. Esser, M. Lai, M. N. Leiske, K. Kempe, G. Sharbeen, J. Youkhana, F. Mansfeld, J. F. Quinn, P. A. Phillips, T. P. Davis, M. Kavallaris and J. A. McCarroll, *Biomaterials*, 2022, **285**, 121539.
- 22 K. Knop, R. Hoogenboom, D. Fischer and U. S. Schubert, *Angew. Chem., Int. Ed.*, 2010, **49**, 6288–6308.
- 23 M. Barz, R. Luxenhofer, R. Zentel and M. J. Vicent, *Polym. Chem.*, 2011, **2**, 1900–1918.
- 24 G. Delaittre, *Eur. Polym. J.*, 2019, **121**, 109281.
- 25 S. Jana and R. Hoogenboom, *Polym. Int.*, 2022, **71**, 935–949.
- 26 M. Glassner, M. Vergaelen and R. Hoogenboom, *Polym. Int.*, 2018, **67**, 32–45.
- 27 B. Guillermin, S. Monge, V. Lapinte and J.-J. Robin, *Macromol. Rapid Commun.*, 2012, **33**, 1600–1612.
- 28 A. Smirnova, T. Kirila, A. Blokhin, N. Kozina, M. Kurlykin, A. Tenkovtsev and A. Filippov, *Eur. Polym. J.*, 2021, **156**, 110637.
- 29 D. Pizzi, A. M. Mahmoud, T. Klein, J. P. Morrow, J. Humphries, Z. H. Houston, N. L. Fletcher, C. A. Bell, K. J. Thurecht and K. Kempe, *Eur. Polym. J.*, 2021, **151**, 110447.
- 30 G. Morgese, L. Trachsel, M. Romio, M. Divandari, S. N. Ramakrishna and E. M. Benetti, *Angew. Chem., Int. Ed.*, 2016, **55**, 15583–15588.
- 31 G. Morgese, B. Verbraeken, S. N. Ramakrishna, Y. Gombert, E. Cavalli, J.-G. Rosenboom, M. Zenobi-Wong, N. D. Spencer, R. Hoogenboom and E. M. Benetti, *Angew. Chem., Int. Ed.*, 2018, **57**, 11667–11672.
- 32 M. N. Leiske, M. Lai, T. Amarasena, T. P. Davis, K. J. Thurecht, S. J. Kent and K. Kempe, *Biomaterials*, 2021, **274**, 120843.

- 33 M. Wang, O. J. R. Gustafsson, G. Siddiqui, I. Javed, H. G. Kelly, T. Blin, H. Yin, S. J. Kent, D. J. Creek, K. Kempe, P. C. Ke and T. P. Davis, *Nanoscale*, 2018, **10**, 10863–10875.
- 34 R. W. Moreadith, T. X. Viegas, M. D. Bentley, J. M. Harris, Z. Fang, K. Yoon, B. Dizman, R. Weimer, B. P. Rae, X. Li, C. Rader, D. Standaert and W. Olanow, *Eur. Polym. J.*, 2017, **88**, 524–552.
- 35 J. Kronek, E. Paulovičová, L. Paulovičová, Z. Kroneková and J. Luston, in *Practical Applications in Biomedical Engineering*, ed. O. A. Adriano, P. Adriano Alves, L. M. N. Eduardo and B. S. Alcimar, IntechOpen, Rijeka, 2013, ch. 11.
- 36 R. Luxenhofer, Y. Han, A. Schulz, J. Tong, Z. He, A. V. Kabanov and R. Jordan, *Macromol. Rapid Commun.*, 2012, **33**, 1613–1631.
- 37 T. Lorson, M. M. Lübtow, E. Wegener, M. S. Haider, S. Borova, D. Nahm, R. Jordan, M. Sokolski-Papkov, A. V. Kabanov and R. Luxenhofer, *Biomaterials*, 2018, **178**, 204–280.
- 38 O. Sedlacek and R. Hoogenboom, *Adv. Ther.*, 2020, **3**, 1900168.
- 39 A. Zahoranová and R. Luxenhofer, *Adv. Healthcare Mater.*, 2021, **10**, 2001382.
- 40 R. Hoogenboom and H. Schlaad, *Polym. Chem.*, 2017, **8**, 24–40.
- 41 A.-S. Glaive, C. Amiel and G. Volet, *Eur. Polym. J.*, 2022, **179**, 111504.
- 42 P. J. Bouten, K. Lava, J. C. van Hest and R. Hoogenboom, *Polymers*, 2015, **7**, 1998–2008.
- 43 Z. A. I. Mazrad, B. Schelle, J. A. Nicolazzo, M. N. Leiske and K. Kempe, *Biomacromolecules*, 2021, **22**(11), 4618–4632.
- 44 S. Jana and M. Uchman, *Prog. Polym. Sci.*, 2020, **106**, 101252.
- 45 M. A. Boerman, H. L. Van der Laan, J. C. M. E. Bender, R. Hoogenboom, J. A. Jansen, S. C. Leeuwenburgh and J. C. M. Van Hest, *J. Polym. Sci., Part A: Polym. Chem.*, 2016, **54**, 1573–1582.
- 46 B. Verbraeken, B. D. Monnery, K. Lava and R. Hoogenboom, *Eur. Polym. J.*, 2017, **88**, 451–469.
- 47 A. C. Rinkenauer, L. Tauhardt, F. Wendler, K. Kempe, M. Gottschaldt, A. Traeger and U. S. Schubert, *Macromol. Biosci.*, 2015, **15**, 414–425.
- 48 M. A. Mees and R. Hoogenboom, *Macromolecules*, 2015, **48**, 3531–3538.
- 49 P. J. M. Bouten, D. Hertsen, M. Vergaelen, B. D. Monnery, S. Catak, J. C. M. van Hest, V. Van Speybroeck and R. Hoogenboom, *J. Polym. Sci., Part A: Polym. Chem.*, 2015, **53**, 2649–2661.
- 50 J. F. R. Van Guyse, M. N. Leiske, J. Verjans, Y. Bernhard and R. Hoogenboom, *Angew. Chem., Int. Ed.*, 2022, **61**, e202201781.
- 51 M. N. Leiske, Z. A. I. Mazrad, A. Zelcak, K. Wahi, T. P. Davis, J. A. McCarroll, J. Holst and K. Kempe, *Biomacromolecules*, 2022, **23**, 2374–2387.
- 52 S. Huber, N. Hutter and R. Jordan, *Colloid Polym. Sci.*, 2008, **286**, 1653–1661.
- 53 R. Obeid, E. Maltseva, A. F. Thünemann, F. Tanaka and F. M. Winnik, *Macromolecules*, 2009, **42**, 2204–2214.
- 54 R. Obeid, F. Tanaka and F. M. Winnik, *Macromolecules*, 2009, **42**, 5818–5828.
- 55 L. T. T. Trinh, H. M. L. Lambermont-Thijs, U. S. Schubert, R. Hoogenboom and A.-L. Kjøniksen, *Macromolecules*, 2012, **45**, 4337–4345.
- 56 S. Hocine and M.-H. Li, *Soft Matter*, 2013, **9**, 5839–5861.
- 57 N. ten Brummelhuis, C. Secker and H. Schlaad, *Macromol. Rapid Commun.*, 2012, **33**, 1690–1694.
- 58 M. M. Bloksma, D. J. Bakker, C. Weber, R. Hoogenboom and U. S. Schubert, *Macromol. Rapid Commun.*, 2010, **31**, 724–728.
- 59 K. Bebis, M. W. Jones, D. M. Haddleton and M. I. Gibson, *Polym. Chem.*, 2011, **2**, 975–982.
- 60 S. Z. Moghaddam and E. Thormann, *J. Colloid Interface Sci.*, 2019, **555**, 615–635.
- 61 P. Patidar and A. Bahadur, *J. Mol. Liq.*, 2018, **249**, 219–226.
- 62 M. M. Lübtow, L. C. Nelke, J. Seifert, J. Kühnemundt, G. Sahay, G. Dandekar, S. L. Nietzer and R. Luxenhofer, *J. Controlled Release*, 2019, **303**, 162–180.
- 63 M. N. Leiske, J. A. Walker, A. Zia, N. L. Fletcher, K. J. Thurecht, T. P. Davis and K. Kempe, *Polym. Chem.*, 2020, **11**, 2799–2810.
- 64 M. M. Lübtow, L. Hahn, M. S. Haider and R. Luxenhofer, *J. Am. Chem. Soc.*, 2017, **139**, 10980–10983.
- 65 P. Ma and R. J. Mumper, *J. Nanomed. Nanotechnol.*, 2013, **4**, 1000164.
- 66 M. Hartlieb, T. Bus, J. Kübel, D. Pretzel, S. Hoepfener, M. N. Leiske, K. Kempe, B. Dietzek and U. S. Schubert, *Bioconjugate Chem.*, 2017, **28**, 1229–1235.
- 67 K. Priyadarshini and A. U. Keerthi, *Med. Chem.*, 2012, **2**, 139–141.
- 68 S. K. Samal, M. Dash, S. Van Vlierberghe, D. L. Kaplan, E. Chiellini, C. van Blitterswijk, L. Moroni and P. Dubruel, *Chem. Soc. Rev.*, 2012, **41**, 7147–7194.